Collisional Stability of Double Bose Condensates

P. S. Julienne, F. H. Mies, E. Tiesinga, and C. J. Williams*

Atomic Physics Division, National Institute of Standards and Technology, Gaithersburg, Maryland 20899

(Received 13 November 1996)

This paper presents quantitative calculations of collisional loss rates for pure ^{23}Na or ^{87}Rb atoms in a binary mixture of hyperfine states $|F, M\rangle$. We find that the recent observation of a dual Bose condensate consisting of ^{87}Rb $|1, -1\rangle$ and $|2, 2\rangle$ atoms is unique and will not occur in Na. We attribute this to the unexpectedly small inelastic spin-exchange rate associated with ^{87}Rb *s*-wave hyperfine collisions. This fortuitous result arises from nearly equal (5.45 ± 0.26 nm) scattering lengths for two colliding ^{87}Rb atoms in their $|1, -1\rangle$ or $|2, 2\rangle$ states. [S0031-9007(97)02586-6]

PACS numbers: 34.50.Pi, 05.30.Jp, 32.80.Pj

The remarkable achievement of Bose-Einstein condensation (BEC) in weakly interacting atomic systems [1,2] has led to widespread interest in the measurement and theory of condensate properties. Ho and Shenoy [3] recently presented a mean field treatment within the Thomas-Fermi approximation for binary mixtures of Bose condensates. The formation of a binary mixture makes possible experimental studies on interpenetrating superfluids and their phase separation. Myatt *et al.* [4] have produced a dual condensate consisting of the $|F = 1, M = -1\rangle$ and $|F = 2, M = 2\rangle$ hyperfine states of ^{87}Rb atoms by using sympathetic cooling of one hyperfine component by the other. The existence of a large, stable condensate of a *single* component requires a positive scattering length for elastic collisions of the identical species, as well as a small inelastic collisional destruction rate. Effective sympathetic cooling requires that the elastic collision rate for momentum transfer between the two components is large, and that the inelastic collision rate that converts either component to an untrapped species is small. Myatt *et al.* [4] measured the inelastic destruction rate coefficient between the two components to be surprisingly small, $2.2 \pm 0.9 \times 10^{-14}$ cm^3/s.

Collisions between ground state alkali atoms take place on two molecular potentials $V_S(R)$: one associated with the $X^1\Sigma_g^+$ state with total electron spin $S = 0$, and one associated with the $a^3\Sigma_u^+$ state with $S = 1$. At ultracold temperatures these potentials are characterized by a pair of scattering lengths A_S, which are crucial in determining the magnitude of the elastic and inelastic collision rates. The scattering length is a measure of the low energy phase shift, $\eta = -kA_S$, of the asymptotic wave, $\sin(kR + \eta)$, for two interacting atoms, relative to the phase, kR, of two noninteracting atoms; here k is the relative momentum of the separated atoms. This paper presents quantum scattering calculations which show the inelastic rate coefficients for Na and for ^{87}Rb as a function of the scattering lengths. We also introduce a model which explains why the loss rates for hyperfine transitions due to spin-exchange collisions is minimized when the singlet A_0 and triplet A_1 scattering lengths are almost equal. Given the experimental constraints on the scattering lengths and inelastic destruction rate for ^{87}Rb, we find that Nature has provided a happy confluence of these two lengths. This suggests that there is a serendipitous reason why sympathetic cooling and dual condensates have been observed for ^{87}Rb. Burke *et al.* [5] have come to a similar conclusion. Our estimates suggest that no such fortuitous agreement exists between the scattering lengths in Na, and thus high inelastic collisional loss rates will occur.

Na and ^{87}Rb both have a nuclear spin of $3/2$ and ground hyperfine levels with $F = 1$ and 2. The $|F = 1, M = -1\rangle$ and $|F = 2, M = 2\rangle$ states, hereafter designated the lower L and upper U states, respectively, are both "weak field seeking" states that can be trapped in a magnetic field with a local minimum. For atom traps used in BEC, a small bias field on the order of 10^{-4} T is present. This field is weak enough that the zero-field limit quantum numbers are approximately good. In addition, at BEC temperatures, only *s*-wave collisions with relative atomic angular momentum equal to zero contribute to the collision rate. $U + U$ elastic collisions occur on the $a^3\Sigma_u^+$ potential and thus $A_{UU} = A_1$. A_1 is measured to be $(109 \pm 10)a_0$ for ^{87}Rb [6] ($1a_0 = 0.052\,917\,7$ nm) and is calculated for Na to be $106^{+79}_{-30}a_0$ [7] and $(85 \pm 3)a_0$ [8]. In contrast, the scattering length A_{LL} for $L + L$ collisions depends on both the $a^3\Sigma_u^+$ and $X^1\Sigma_g^+$ potential, and generally is not equal to either A_0 or A_1. A_{LL} is measured to be $(87 \pm 21)a_0$ for ^{87}Rb [9] and $(52 \pm 5)a_0$ for Na [8].

Inelastic collisions occur by two distinct physical mechanisms which have different selection rules: spin-exchange interactions or spin-dipole interactions [10]. The spin-exchange mechanism is inherently strong, depending on the chemical exchange force that splits the $a^3\Sigma_u^+$ and $X^1\Sigma_g^+$ molecular potentials as the charge clouds of the two atoms overlap. At zero magnetic field spin-exchange transitions are only possible if the following quantum numbers are conserved: the relative angular momentum ℓ of the two atoms, the resultant spin angular momentum f of the two atoms a and b,

 0031-9007/97/78(10)/1880(4)$10.00

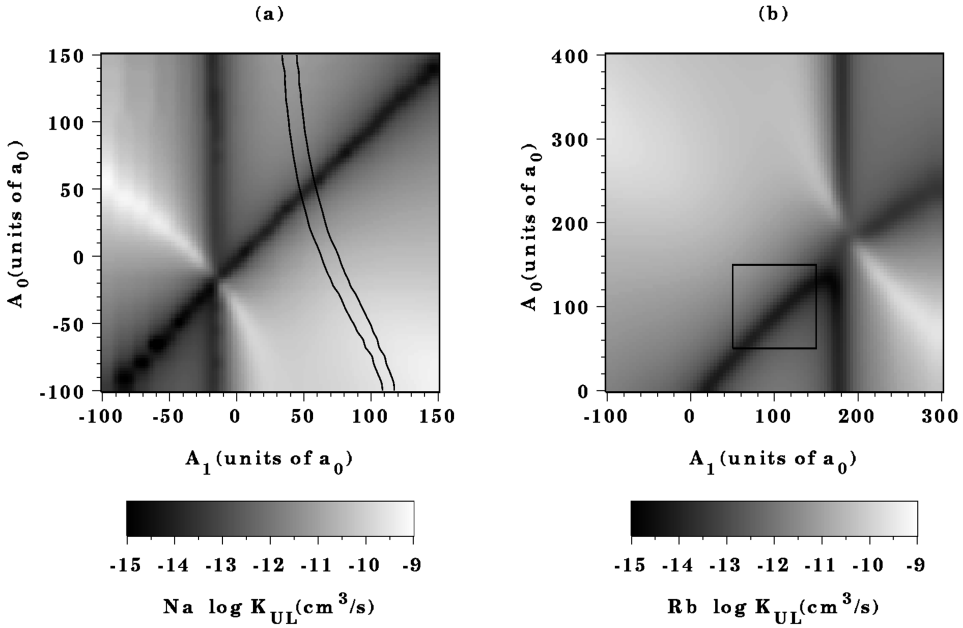

FIG. 1. $K_{UL}(A_0, A_1)$ versus A_0 and A_1 at zero magnetic field for (a) Na and for (b) ^{87}Rb. The gray scale is logarithmic, ranging from a maximum (white) 10^{-9} cm^3/s to a minimum (black) 10^{-15} cm^3/s. The approximately parallel lines for Na bracket the region where the calculated $L + L$ scattering length A_{LL} varies between $47a_0$ and $57a_0$, consistent with Ref. [8]. The box for Rb is expanded in Fig. 3.

where $f = F_a + F_b$, and the projection m of f on the space fixed axis, $m = M_a + M_b$. On the other hand, the spin-dipole mechanism is inherently weak, depending on relativistic spin-dependent forces proportional to the square of the fine-structure constant. For an entrance channel s wave, spin-dipolar transitions require a d-wave ($\ell = 2$) exit channel. Collisions which change f, m, and/or ℓ only occur by the spin-dipolar mechanism, and consequently have rate coefficients on the order of 10^{-15} cm^3/s [10,11].

Inelastic collision rates for $U + U$ or $L + L$ involve *only* the weak spin-dipolar mechanism and thus tend to be small in alkali traps, permitting trap lifetimes of 10 s or longer. On the other hand, the inelastic collisions of $L + U$ can occur by the strong spin-exchange mechanism, where a rate coefficient exceeding 10^{-10} cm^3/s is possible. This naturally raises the question as to why this observed rate coefficient in ^{87}Rb is so small.

We use standard close coupling techniques to calculate rate coefficients for any pair of collision partners $(F_a M_a, F_b M_b)$ going to any other pair $(F'_a M'_a, F'_b M'_b)$ [8,10,11]. We carried out calculations to verify that a 10^{-4} T bias field does not modify our conclusions, and thus we present results in the limit of zero field. The calculations are based upon the atomic hyperfine interaction of each atom, the rotation of the nuclei about their center of mass, the spin-spin magnetic dipole interaction, the second-order spin-orbit interaction for ^{87}Rb [11], and the adiabatic Born-Oppenheimer potentials for the $X^1\Sigma_g^+$ and $a^3\Sigma_u^+$ states. Although the potentials are well characterized at long range, there are uncertainties associated with the short range chemical bonding region. We adjust the inner region of these potentials [8,11] in order to study the effects the uncertainties have on the scattering lengths, and thus the collision rates.

To give a picture of the topology of $K_{UL}(A_0, A_1)$ [12], the sum of all inelastic collision rate coefficients (including depolarization) for removing U and L atoms from the trap due to a $U + L$ collision ($\dot{n}_U = \dot{n}_L = -K_{UL} n_U n_L$, where n indicates density), we varied A_0 and A_1 over a range that greatly exceeds their experimental uncertainties. Figure 1 summarizes our calculations for $K_{UL}(A_0, A_1)$ at a collision energy of 100 nK for both ^{87}Rb and Na. This represents a thermally averaged rate, since K_{UL} is independent of collision energy at BEC temperatures [10]. Although contributions from both spin-exchange and spin-dipolar mechanisms are included, K_{UL} is dominated by the spin-exchange contribution, except possibly at the low end of its range near 10^{-15} cm^3/s. K_{UL} includes the depolarization processes, $U + L \rightarrow |F = 2, M = 1\rangle + |F = 1, M = 0\rangle$ and $U + L \rightarrow |F = 2, M = 0\rangle + |F = 1, M = 1\rangle$. Although depolarization processes are suppressed at zero magnetic field due to threshold properties of the exit channel, they lead to a factor of 3 increase in K_{UL} at 10^{-4} T.

The two panels in Fig. 1 show a strikingly similar topology that can be explained in terms of the basic physics of these collisions. The figure shows two narrow dark bands corresponding to small rate coefficients on the order of 10^{-14} cm^3/s. One band runs diagonally, and corresponds to the case where A_0 and A_1 are nearly equal. The second band runs vertically, independent of A_0. This general topology repeats itself as one adds or removes bound states from the $X^1\Sigma_g^+$ and the $a^3\Sigma_u^+$ potentials [11].

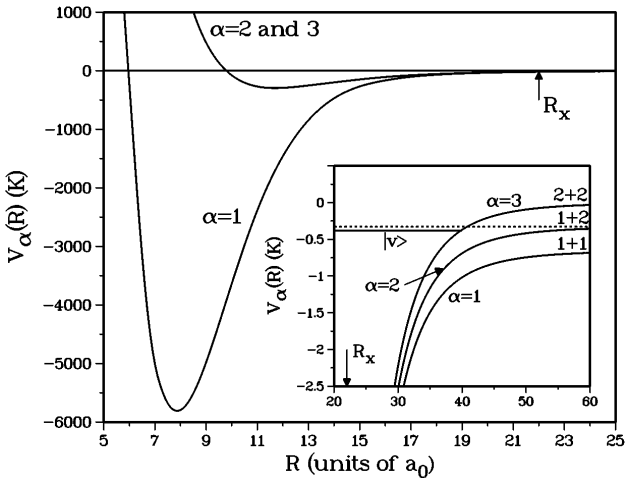

FIG. 2. Adiabatic potentials for ^{87}Rb for the 3×3 model of s-wave exchange scattering for $F_{\rm tot} = f = 2$. The inset shows the potentials for $R > R_x$ [$V_\alpha(R_x) \approx -16$ K], where the dotted line represents a 100 nK $L + U$ collision. The solid line labeled $|v\rangle$ represents the location of a bound state (Feshbach resonance) for the $\alpha = 3$ potential that is consistent with all experimental data. A $|v\rangle$ that is degenerate with the dotted line gives rise to the dark vertical bands shown in Fig. 1.

Over most of the plane in Fig. 1(b), K_{UL} is larger by one or more orders of magnitude than the measured value of 2.2×10^{-14} cm^3/s for ^{87}Rb [4].

A simple three-channel, zero magnetic field, model Hamiltonian explains the existence of the vertical and diagonal bands [11]. In this model, the total angular momentum $F_{\rm tot}$ is a good quantum number and we can use a total angular momentum basis, $|(F_a F_b) f \ell F_{\rm tot}\rangle$ for our calculations [8,11]. Furthermore, only $F_{\rm tot} = 2$ contributes to s-wave spin-exchange $U + L$ collisions and only three $F_{\rm tot} = f = 2$ s-wave channels exist. They represent the atomic states $(F_a F_b) = (22)$, (21), and (11), and are strongly coupled by the exchange interaction. In this model K_{UL} equals the rate coefficient for scattering from $(F_a F_b) = (21)$ to $(F_a F_b) = (11)$. Figure 2 shows the three adiabatic potentials $\alpha = 1$, 2, and 3 for ^{87}Rb found from diagonalizing the 3×3 interaction matrix. For $R \gg R_x$, these three potentials are parallel, have the same van der Waals potential $-C_6/R^6$, and are separated by the atomic hyperfine splitting. Here R_x is the distance where the R-dependent exchange splitting equals the hyperfine splitting. For $R \ll R_x$ the $\alpha = 2$ and 3 potentials correlate with the $a^3\Sigma_u^+$ potential, and the lowest potential correlates with the $X^1\Sigma_g^+$ potential. Note that at R_x ($22a_0$ for ^{87}Rb and $21a_0$ for Na) the binding energy of the three potentials is large compared to the exchange and hyperfine splittings. Moreover, both splittings are very large compared with the entrance channel collision energy.

The diagonal and vertical bands in Fig. 1 result from two distinct ways by which K_{UL} can become small. The diagonal band occurs because of phase matching near R_x between the incoming wave function in channel 2 and the outgoing wave function in channel 1. The adiabatic potentials near R_x are so deep (several K) that the accelerated atoms move through the region near R_x quickly and the motion need not be adiabatic. In fact, the adiabatic channels are strongly coupled by the operator $O_{12} = (\mathbf{M}^t d\mathbf{M}/dR)_{12} d/dR$ [11], where $\mathbf{M}$ is the 3×3 matrix that diagonalizes the 3×3 interaction matrix. The coupling matrix element $(\mathbf{M}^t d\mathbf{M}/dR)_{12}$ is strongly localized within a few a_0 around R_x, and the probability of the spin-exchange transition from channel 2 to 1 is proportional to the square of the matrix element $\langle \Psi_1 | O_{12} | \Psi_2 \rangle$. The scattering wave functions for the adiabatic channels, Ψ_i, are proportional to $\sin \beta_i(R)$, $i = 1, 2$, where $\beta_i(R)$ represents the phase accumulated up to R. Thus, because of the d/dR operator this matrix element will be *minimal* when the two wave functions are nearly *in phase*, $\beta_1(R_x) \approx \beta_2(R_x)$, in the strong coupling region. Because of the depth of the potentials at R_x, the $\beta_i(R_x)$ are nearly independent of collision energy over an energy range comparable to the atomic hyperfine splitting. Additionally, since the potentials between R_x and ∞ are nearly parallel (see Fig. 2), the phase picked up between R_x and ∞ will be almost the same for the two channels when the asymptotic kinetic energies are the same. As a result, all scattering lengths, including A_{LL}, A_1, and A_0, are approximately equal. This is the condition that causes the diagonal band of low K_{UL} in Fig. 1.

The vertical band in Fig. 1 is a resonance effect which results when the bound state $|v\rangle$ of the $\alpha = 3$ potential (see Fig. 2) happens to coincide with the $U + L$ collision energy. The vertical band depends only on A_1 because the $\alpha = 3$ potential is essentially the $a^3\Sigma_u^+$ potential. In other words, by adjusting A_1 it is possible to place a bound state (resonance) at the $U + L$ ($\alpha = 2$) collision threshold. In this case, there is an interference between the direct path, $\alpha = 2 \rightarrow \alpha = 1$, and the indirect path, $\alpha = 2 \rightarrow \alpha = 3$ (resonance) $\rightarrow \alpha = 1$. For Na, the resonance in question is the last bound state in the $\alpha = 3$ potential, whereas for ^{87}Rb it is the fourth from the last bound state. The Eindhoven group [13] has proposed that these resonances can be moved using a magnetic field so that a desired scattering length can be selected. A magnetic field can also shift the resonance close to threshold, thereby suppressing inelastic rates. However, the $\approx 10^{-4}$ T field in current traps will not move the vertical bands perceptibly in Fig. 1.

Figure 3 presents K_{UL} for ^{87}Rb at zero magnetic field in the experimentally relevant domain of parameter space. The rate coefficient K_{UL}, A_{UU}, and A_{LL} all lie within their experimental uncertainty [14] in the hashed area of Fig. 3. Clearly, for all experimental data to be consistent, A_{UU} and A_{LL} must be more similar then current experimental measurements suggest. The hyperfine splitting of ^{87}Rb ensures that the minimum value of K_{UL} *does not* exist for $A_0 = A_1$ ($= A_{UU}$) but actually has its minimum when $A_0 \approx A_1 - 10a_0$. In Na, the hyperfine interaction is smaller, and the corresponding shift is only $2a_0$.

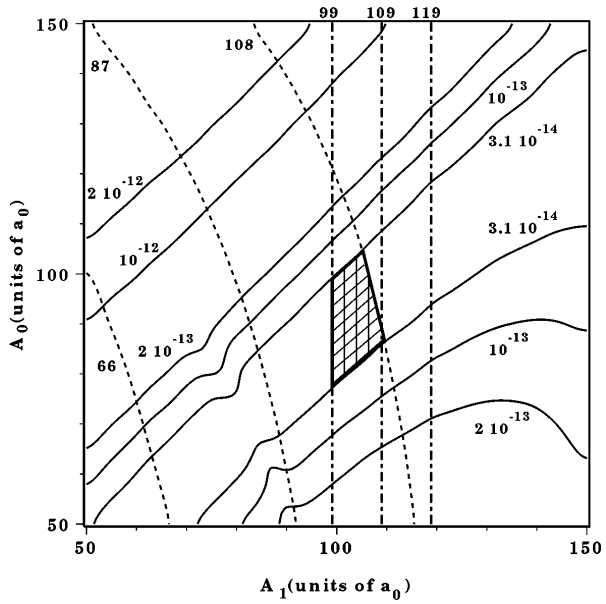

FIG. 3. A blowup of the boxed region of Fig. 1(b) for ^{87}Rb. The solid contours show K_{UL} on a log scale. The contour 3.1×10^{-14} cm^3/s is the upper limit of the measured K_{UL} [4]. The dashed lines are calculated lines of constant A_{LL} showing its experimental range of $(87 \pm 21)a_0$ [9]. The vertical dot-dashed lines show the measured experimental range for $A_{UU} = A_1 = (109 \pm 10)a_0$ [6].

When the inelastic K_{UL} is sufficiently small, it is legitimate to parametrize $U + L$ *elastic* collisions by a real scattering length A_{UL}, as used by Ho and Shenoy [3]; in general, A_{UL} would have a large imaginary component due to inelastic collisions. We find that in the hashed region of Fig. 3 our calculated values of A_{LL}, A_{UU}, and A_{UL} all lie in the range $(103 \pm 5)a_0$. Moreover, the three scattering lengths are correlated, never differing by more than $4a_0$ from one another. A magnetic field of 10^{-4} T causes an increase in the calculated rate coefficient K_{UL}, and thus the hashed region is a conservative estimate for the regime where all data are consistent.

Our calculations also constrain the range of other inelastic rate coefficients. In the diagonal band, all spin-exchange inelastic rate coefficients are small, for example, for collisions of U with $|F = 2, M \neq 2\rangle$ states. The hashed area of Fig. 3 constrains the zero-field spin-dipolar loss rate coefficient K_{UU} for $U + U$ collisions ($\dot{n}_U = -K_{UU} n_U^2$) [11] to lie between 0.4×10^{-15} cm^3/s and 0.7×10^{-15} cm^3/s. At 10^{-4} T, this rate coefficient is increased by a factor of 3. Thus, the ^{87}Rb spin-dipolar K_{UU} should lie in the range $(1 - 2) \times 10^{-15}$ cm^3/s in a typical magnetic trap for BEC.

The inelastic rates for Na provide a strong contrast to ^{87}Rb. The lines on Fig. 1(a) show the constraint provided by the uncertainty in $A_{LL} = (52 \pm 5)a_0$ [8]. The published values of A_1, 106^{+79}_{-30} [7] and $(85 \pm 3)a_0$ [8], are derived from theory and constrain K_{UL} to a region having the order of magnitude 10^{-10} cm^3/s. Our preliminary analysis of recent unpublished photoassociation data for $(F_a F_b) = (22)$ and (21) collisions suggests that our error range for A_1 [8] may be overly optimistic; however, it will not qualitatively change this result. Quantitative constraints on inelastic rate coefficients for Na depend on better experimental constraints on A_1. Large inelastic rate coefficients on the order of 10^{-10} cm^3/s will cause rapid depletion of trapped species and severely limit the prospects of evaporative and sympathetic cooling.

In conclusion, the spin-exchange inelastic collision rates are unusually small for ^{87}Rb because of a special coincidence of A_0 and A_1. We calculate these rates to be so large in Na that dual condensates of U and L species are unlikely. A similar statement will apply for other alkali systems with unequal scattering lengths, unless there are threshold resonances as described above. Dual condensates may be possible between mixed species/isotopes when *both* species/isotopes are in low-field seeking states of the lower hyperfine manifold (or in the doubly polarized state). The collisional loss rates go via a dipolar mechanism, for example, a dual condensate of ^{87}Rb $|F = 1, M = -1\rangle$ and Na $|F = 1, M = -1\rangle$.

*Permanent address: James Franck Institute, University of Chicago, Chicago, IL 60637.

[1] M. H. Anderson *et al.*, Science **269**, 198 (1995).
[2] K. B. Davis *et al.*, Phys. Rev. Lett. **75**, 3969 (1995).
[3] Tin-Lun Ho and V. B. Shenoy, Phys. Rev. Lett. **77**, 3276 (1996).
[4] C. J. Myatt, E. A. Burt, R. W. Ghrist, E. A. Cornell, and C. E. Wieman , Phys. Rev. Lett. **78**, 586 (1997).
[5] J. P. Burke, Jr., J. L. Bohn, B. D. Esry, and C. H. Greene Phys. Rev. A (to be published).
[6] H. M. J. M. Boesten, C. C. Tsai, J. R. Gardner, D. J. Heinzen, and B. J. Verhaar, Phys. Rev. A **55**, 636 (1997).
[7] A. J. Moerdijk and B. J. Verhaar, Phys. Rev A **51**, R4333 (1995).
[8] E. Tiesinga *et al.*, J. Res. Natl. Inst. Stand. Technol. **101**, 505 (1996).
[9] N. Newbury, C. Myatt, and C. Wieman [Phys. Rev. A **51**, R2680 (1995)] reported the absolute value of A_{LL}. The sign is inferred from the observation of a large condensate for ^{87}Rb $|1, -1\rangle$ atoms in Ref. [4].
[10] H. T. C. Stoof, J. M. V. A. Koelman, and B. J. Verhaar, Phys. Rev. B **38**, 4688 (1988).
[11] F. H. Mies *et al.*, J. Res. Natl. Inst. Stand. Technol. **101**, 521 (1996).
[12] This rate coefficient is for a Maxwellian gas; it is modified by a factor of $(2 - \xi^2)/2$ if a condensate is present with fraction ξ [see H. T. C. Stoof *et al.*, Phys. Rev. A **39**, 3157 (1989)].
[13] E. Tiesinga, B. J. Verhaar, and H. T. C. Stoof, Phys. Rev. A **47**, 4114 (1993); A. J. Moerdijk and B. J. Verhaar, Phys. Rev. Lett. **73**, 518 (1994).
[14] The $\pm 21a_0$ error limit for A_{LL} [9] is a 2σ limit [C. J. Myatt (private communication)]; the $\pm 10a_0$ error limit for A_{UU} represents a 90% confidence level.